

# Fluid-crystal coexistence for proteins and inorganic nanocolloids: dependence on ionic strength

Peter Prinsen and Theo Odijk\*,  
*Complex Fluids Theory, Faculty of Applied Sciences,  
Delft University of Technology, Delft, the Netherlands*

We investigate theoretically the fluid-crystal coexistence of solutions of globular charged nanoparticles like proteins and inorganic colloids. The thermodynamic properties of the fluid phase are computed via the optimized Baxter model. This is done specifically for lysozyme and silicotungstates for which the bare adhesion parameters are evaluated via the experimental second virial coefficients. The electrostatic free energy of the crystal is approximated by supposing the cavities in the interstitial phase between the particles are spherical in form. In the salt-free case a Poisson-Boltzmann equation is solved to calculate the effective charge on a particle and a Donnan approximation is used to derive the chemical potential and osmotic pressure in the presence of salt. The coexistence data of lysozyme and silicotungstates are analyzed within this scheme, especially with regard to the ionic-strength dependence of the chemical potentials. The latter agree within the two phases provided some upward adjustment of the effective charge is allowed for.

\*Address for correspondence: T. Odijk, P.O. Box 11036, 2301 EA Leiden, the Netherlands  
E-mail: odijktcf@wanadoo.nl

## I. INTRODUCTION

One current view of protein crystallization centers on the second virial coefficient  $B_2$  being a relevant quantity determining the onset of crystallization [1, 2, 3, 4]. There exists a crystallization slot of negative  $B_2$  values which expresses a necessary range of solution conditions for adequate crystals to grow. A negative value of  $B_2$  implies a Baxter stickiness parameter as it is conventionally defined and we here denote by  $\tau_0$ . Thus, in a similar vein,  $\tau_0$  has been correlated with the solubility of nanoparticles in explaining fluid-crystal coexistence curves [5, 6].

The free energy of a suspension of particles cannot, of course, depend on  $B_2$  alone. In a recent paper [7] we introduced a new analytical theory for protein solutions in which the real fluid is replaced by a suspension of spheres with an appropriately chosen adhesion of the Baxter type. The stickiness parameter  $\tau$  in the latter is computed by a variational principle for the free energy. In our optimized Baxter model,  $\tau$  is not at all identical to  $\tau_0$  but depends not only on the ionic strength but also on the protein concentration. In Ref. [5], Rosenbaum et al. plotted  $\tau_0$  logarithmically as a function of the nanoparticle concentration which effectively coarse-grains the experimental data they show. If we zoom in on their curve, there is a lot of fine detail which we here argue to be related to the fact that  $\tau$  is a better similarity parameter. In particular, we seek to understand the ionic-strength dependence of the fluid-crystal coexistence curves by going beyond theory based solely on  $\tau_0$ .

We have recently tested the optimized Baxter model on a system of spheres interacting via an attractive Yukawa potential analyzed by computer simulations [8]. The stickiness parameter  $\tau$ , evaluated by optimizing the free energy, is indeed a useful similarity variable for gaining insight into the pressures and chemical potentials from the simulations. The magnitudes of these quantities are also well predicted by the optimized Baxter model.

However, here we will not focus on the variable  $\tau$  and the fluid phase but rather on the coexistence itself. The systems we study are assumed to have a short enough range so that the coexistence between two fluid phases is circumvented. An a priori theory is problematic because we would need a quantitative theory of the crystal phase in terms of postulated attractive forces which are currently unknown. Theoretical efforts exist in the literature [9, 10, 11] at the expense of introducing unknown parameters which we want to avoid here.

In practice, it may be very difficult to achieve ideal thermodynamic equilibrium between the liquid phase and some crystalline state. Equilibrium may not have been reached, the crystal could be heterogeneous and the formation of aggregates could complicate the attainment of equilibrium (see, for instance, the discussion by Cacioppo and Pusey on lysozyme [12]). Nevertheless, it may still be useful to assume equilibrium is ideally attained provided our goal is sufficiently modest. The balance of chemical potentials has been used before to acquire information about the crystal from the solubility in the fluid phase [3]. Our concern here will be to try to gain insight into the ionic-strength dependence of the thermodynamic properties of the crystal. We may argue that this dependence could be approximated by a Donnan equilibrium so it would not be very sensitive to the precise crystal habit adopted. We therefore compute the protein chemical potential and osmotic pressure of the coexisting liquid phase at the experimentally determined solubility with the help of the optimized Baxter model. We then investigate whether their dependence on the electrolyte concentration agrees with that predicted by a simple crystal model.

## II. OPTIMIZED BAXTER MODEL

We first discuss how we obtain the bare adhesion parameters via the second virial coefficient, and then summarize the optimized Baxter model which is a liquid state theory at finite concentrations [7]. We consider a system of charged nanometer-sized particles (e.g. proteins or nanocolloids) in water with added monovalent salt of ionic strength  $I$ . We suppose the particles are spherical with radius  $a$ . The charge is distributed uniformly on the particle's surface. For convenience, all distances in this section will be scaled by the radius  $a$  and all energies by  $k_B T$ , where  $k_B$  is Boltzmann's constant and  $T$  is the temperature. Because monovalent ions (counterions and salt ions) are present in solution, the Coulomb repulsion between the particles will be screened and it is here given by a far-field Debye-Hückel potential [7]. The effective number  $Z_{eff}$  of charges on the sphere (taken to be positive) will here be computed in the Poisson-Boltzmann approximation. We let the attraction between two particles be of range much shorter than their radius, and we model it by a potential well of depth  $U_A$  and width  $\delta \ll 1$ . The total interaction  $U(x)$  between two particles whose centers of mass are separated by an actual distance  $r$  is thus of the form

$$U(x) = \begin{cases} \infty & 0 \leq x < 2 \\ U_{DH}(x) - U_A & 2 \leq x < 2 + \delta \\ U_{DH}(x) & x \geq 2 + \delta \end{cases}, \quad (1)$$

$$x \equiv \frac{r}{a},$$

with Debye-Hückel interaction

$$U_{DH}(x) = 2\xi \frac{e^{-\omega(x-2)}}{x}. \quad (2)$$

Here,  $\xi \equiv \frac{Q}{2a} \left( \frac{Z_{eff}}{1+\omega} \right)^2$  and  $\omega \equiv \kappa a$ , which are given in terms of the Debye length  $\kappa^{-1}$  defined by  $\kappa^2 = 8\pi QI$  and the Bjerrum length  $Q = q^2/\epsilon k_B T$ , which equals 0.71 nm in water at 298 K ( $\epsilon$  is the permittivity of water,  $q$  is the elementary charge);  $\omega = 3.28a\sqrt{I}$ , if the radius  $a$  is given in nm and the ionic strength  $I$  in M. We suppose 1-1 electrolyte has been added in excess so  $I$  is the concentration of added salt. We have derived the effective charge  $qZ_{eff}$  in the Poisson-Boltzmann approximation [7]

$$Z_{eff} = Z - \frac{\omega^2}{6} \left( \frac{Q}{a} \right)^2 \left( \frac{Z}{1+\omega} \right)^3 e^{3\omega} E_1(3\omega). \quad (3)$$

Here  $E_1(x)$  is the exponential integral defined by  $E_1(x) = \int_x^\infty dt t^{-1} e^{-t}$  and  $qZ$  is the actual charge per particle.

We suppose that the bare charge on the particles as a function of the ionic strength is known from experiment, so the only unknown parameters are  $U_A$  and  $\delta$  which are chosen to be independent of  $I$ . The latter are determined by fitting preferably complete experimental data of the second virial coefficient  $B_2$  as a function of the ionic strength  $I$  at constant pH to  $B_2$  computed numerically with the help of the expression

$$B_2 = 2\pi a^3 \int_0^\infty x^2 dx \left( 1 - e^{-U(x)} \right) \quad (4)$$

using Eq. (1). We have previously done this for a wide variety of  $B_2$  data on lysozyme at two values of the pH (4.5 and 7.5) and we were able to obtain very good fits [7] (see e.g. Fig. 1 which is discussed in section III.B).

It is important to stress that though there are two adjustable parameters  $\delta$  and  $U_A$ , the actual fit in practice depends almost solely on adjusting the single combination  $\delta \exp U_A$ . This is because a convenient analytical approximation of the second virial turns out to have the form [7]

$$\frac{B_2}{B_2^{HS}} \simeq 1 + \frac{3\xi}{2\omega} - \frac{3}{2} e^{-\xi} \delta e^{U_A} \quad (5)$$

and is able to describe the experimental data on lysozyme quite well with an appropriate value of  $\delta \exp U_A$ . Here,  $B_2^{HS}$  is the second virial coefficient pertaining to hard spheres. We note that Eq. (5) disagrees starkly with an approximation put forward earlier [13], both with regard to the pure electrostatic and the adhesive contributions. In particular, the third i.e. adhesion term in Eq. (5) is not at all independent of the ionic strength but rather diminishes fast as the electrolyte concentration is lowered. Furthermore, the pure electrostatic term cannot be derived from a Donnan equilibrium as we point out in Section IV.

At high salt concentrations, the parameter  $\xi$  becomes small owing to screening so  $B_2$  becomes lower than the hard sphere value as can be seen from Eq. (5). Nevertheless, the electrostatic repulsion still exerts itself, so an effective adhesion parameter we may wish to introduce would be smaller than the bare value. We therefore adopt a similar strategy to the liquid state at finite concentrations by first introducing a suitable reference state amenable to analytical computation [7]. This is a solution of hard spheres whose radius is still  $a$  but with a Baxter adhesion potential whose strength is defined by a suitable stickiness parameter  $\tau$ . The statistical properties of this suspension as a function of the volume fraction of spheres  $\eta$  ( $= 4\pi a^3/3$  times number density) may be solved in the Percus-Yevick approximation [14]. The parameter  $\tau$  is adjustable and is computed via a variational principle for the free energy. The latter may be written as a functional expansion in terms of the so-called blip function which is the difference in Mayer functions of the respective interactions (Eq. (1) and the Baxter interaction) [7, 15]. We set the first-order deviation from the free energy pertaining to the reference state equal to zero. This determines  $\tau$  which depends not only on the well parameters  $\delta$  and  $U_A$  and electrostatic variables  $\omega$  and  $\xi$  but also on the volume fraction of nanospheres. It is given by [7]

$$\frac{1}{\tau} = 3\epsilon \left[ \left( e^{U_A} e^{-\frac{\xi}{1+\epsilon/2}} e^{-\omega\epsilon} - 1 \right) (1 + (1+H)\epsilon) + (e^{U_A} e^{-\xi} - 1) \right], \quad (6)$$

where

$$\epsilon = \delta - K^{-1} [(1 + \delta H)P_1 + HP_2], \quad (7)$$

$$P_1 = \frac{8}{\omega^2} (1 + \omega\delta)M + \frac{16}{\omega} \left( \frac{M}{1+M} \right), \quad (8)$$

$$P_2 = \frac{8}{\omega^3} (2 + \omega\delta)M + \frac{16}{\omega^2} \ln(1+M), \quad (9)$$

$$M \equiv \xi e^{-\omega\delta}/4, \quad (10)$$

$$K_1 = 2 \left( e^{U_A} e^{-\frac{\xi}{1+\delta/2}} e^{-\omega\delta} - 1 \right) (1 + (1+H)\delta) + 2 \left( e^{U_A} e^{-\frac{\xi}{1+\epsilon/2}} e^{-\omega\epsilon} - 1 \right) (1 + (1+H)\epsilon), \quad (11)$$

$$H = \frac{\eta}{2\tau(1-\eta)} \left( \frac{\eta(1-\eta)}{12} \lambda^2 - \frac{1+11\eta}{12} \lambda + \frac{1+5\eta}{1-\eta} - \frac{9(1+\eta)}{2(1-\eta)^2} \frac{1}{\lambda} \right) \quad (12)$$

and  $\lambda$  is given by

$$\tau = \frac{1+\eta/2}{(1-\eta)^2} \frac{1}{\lambda} - \frac{\eta}{1-\eta} + \frac{\eta}{12} \lambda. \quad (13)$$

Note that  $\tau$  is readily obtained by iteration. One starts with initial values for  $\tau$  and  $\epsilon$  and then calculates  $\lambda$ ,  $H$  and  $K_1$  from Eqs. (11)–(13). Then, a new value of  $\epsilon$  at fixed  $H$  is computed iteratively with the help of Eqs. (7) and (11). Next, a new value of  $\tau$  is given by Eq. (6) and then the cycle is repeated until the variables become stationary.

Having obtained the effective adhesion parameter  $\tau$ , we simply calculate thermodynamic properties of the reference state within the Percus-Yevick approximation. The free energy of the actual system does deviate slightly from that of the reference state but we have shown that the deviations are very small [7]. To compute the osmotic pressure  $\Pi$  we use the result from the compressibility route [14]

$$\frac{\Pi v_0}{k_B T} = \frac{\eta(1+\eta+\eta^2)}{(1-\eta)^3} - \frac{\eta^2(1+\eta/2)}{(1-\eta)^2} \lambda + \frac{\eta^3}{36} \lambda^3. \quad (14)$$

When the roots of Eq. (13) are complex, the pressure cannot be determined for the physical realization of the liquid state breaks down, at least with the Percus-Yevick approximation. The chemical potential  $\mu$  of the spherical particles is determined by using the pressure from Eq. (14) and the Gibbs-Duhem equation at constant temperature [16]

$$\frac{\mu - \mu_0}{k_B T} = \ln \frac{\eta}{1-\eta} + \frac{3\eta(4-\eta)}{2(1-\eta)^2} + \frac{\Pi v_0}{k_B T} + J. \quad (15)$$

Here

$$J = \frac{3}{2}\eta^2\lambda^2 - \frac{3\eta(1+4\eta)}{(1-\eta)}\lambda + \frac{6\eta(2+\eta)}{(1-\eta)^2} - \frac{18\eta}{1-\eta}\tau - \frac{6(\tau-\tau_c)^2}{\tau_c(1-6\tau_c)} \ln \left| \frac{\lambda(1-\eta) - \tau_c^{-1}}{\tau^{-1} - \tau_c^{-1}} \right| + \frac{6\tau_c(18\tau\tau_c - 1)^2}{1-6\tau_c} \ln \left| \frac{\lambda(1-\eta) - 18\tau_c}{\tau^{-1} - 18\tau_c} \right| \quad (16)$$

is the contribution to the chemical potential that vanishes in the hard-sphere limit ( $\tau \rightarrow \infty$ ) and

$$\frac{\mu_0}{k_B T} = \ln \frac{1}{v_0} \left( \frac{h^2}{2\pi m k_B T} \right)^{3/2} \quad (17)$$

where  $h$  is Planck's constant and  $m$  is the mass of a sphere. The critical value of  $\tau$  below which there is a range of densities where there is no real solution of  $\lambda$ , is given by

$$\tau_c = \frac{2 - \sqrt{2}}{6}. \quad (18)$$

### III. SOLUBILITY CURVES: CHEMICAL POTENTIAL OF THE FLUID PHASES

#### A. Method

Since we suppose the crystal is in thermodynamic equilibrium with the fluid, the protein chemical potentials as well as the osmotic pressures in both phases are uniform. The chemical potential of the counter and co-ions must also be uniform but we will address this issue later within a Donnan equilibrium. Solubility data from experiment represent the particle concentration in the fluid phase as a function of the pH and the salt concentration. Thus we compute the chemical potential and the osmotic pressure of the solution with the help of the optimized Baxter model of the previous section. We have done this in two cases of nanoparticles where we have sufficient experimental data on the second virial coefficient to evaluate the well parameters  $U_A$  and  $\delta$  with sufficient accuracy.

#### B. Lysozyme

The protein hen-egg-white lysozyme has been well characterized in aqueous solutions of simple electrolytes. We here choose the effective radius  $a$  such that the volume of the model sphere is equal to the volume of a lysozyme molecule in the tetragonal crystal state. The latter is determined from the water content of the tetragonal crystal (0.335 mass fraction [17]), the crystal volume per protein molecule (29.7 nm<sup>3</sup> [18]), the density of the crystal (1.242 10<sup>3</sup> kg m<sup>-3</sup> [17]) and the density of water (0.998 10<sup>3</sup> kg m<sup>-3</sup>). Thus we have  $a = 1.61$  nm and note that this is about 0.1 nm less than the value of 1.7 nm we used previously [7], which was based on approximating the protein by an ellipsoid of dimensions 4.5 × 3.0 × 3.0 nm [19]. For the sake of consistency we here use the single value  $a = 1.61$  nm in computations pertaining to both phases.

The experimental data for the second virial coefficient of lysozyme have been discussed by us at length previously [7] and are presented in Fig. 1. For details on determining the parameters  $U_A$  and  $\delta$  of the attractive potential we also refer to Ref. [7]. Since we are using a smaller effective radius here, we deduce the values  $U_A = 2.89$  and  $\delta = 0.182$  which are somewhat different from those derived earlier [7]. The values of the bare charge  $qZ$  of a lysozyme molecule as a function of the ionic strength are the same as those used in Ref. [7] i.e. they are determined by interpolation from hydrogen-ion titration data in KCl [20]. We assume that KCl and NaCl (see below) behave identically in an electrostatic sense. The effective charge does differ slightly because it is a function of  $a$  (see Eq. (3)). We again use the lowered effective charge  $\bar{Z} = Z_{eff} - 1$  instead of the effective charge  $Z_{eff}$  in order to fit  $B_2$  accurately at lower ionic strengths when it is dominated by electrostatics. We set  $U_A$  and  $\delta$  to be independent of the pH.

Accurate data on the solubility  $S$  as a function of the NaCl concentration have been obtained by Cacioppo and Pusey [12] using column beds of tetragonal microcrystallites of lysozyme in a range of pH and temperatures. We here employ their data at 298 K and at three representative values of the pH. (See Tables I, II and III.) The ionic strength  $I$  in M is determined from the ionic strength in %w/v by the relation  $I(\text{M}) = 0.06 + 0.171 I(\%w/v)$ . Here, the value 0.06 accounts for the effective ionic strength of the 0.1 M sodium acetate buffer used and 0.171 = 10/ $M_{NaCl}$  where  $M_{NaCl} = 58.44$  g mol<sup>-1</sup> is the molar mass of NaCl. The dimensionless parameter  $\omega$  is then given by  $\omega = 5.28\sqrt{I}$ , where  $I$  is given in M, and  $\xi = 0.220(\bar{Z}/(1+\omega))^2$ .

The volume fraction  $\eta$  of protein in the liquid phase is given by  $\eta = SN_A v_0/M$ , where  $N_A$  is Avogadro's number,  $v_0 = 4\pi a^3/3$  is the volume of a lysozyme molecule and  $M = 14.3 \text{ kg mol}^{-1}$  [21] is the molar mass of lysozyme. The parameter  $\tau$  describing the effective adhesion is determined as described in section II (see Eqs. (6)–(13)), using the values  $U_A = 2.89$  and  $\delta = 0.182$ . Then, the dimensionless chemical potential  $(\mu - \mu_0)/k_B T$  and the dimensionless osmotic pressure  $\Pi v_0/k_B T$  are determined from Eqs. 15 and 14 respectively. (See Tables I, II and III). Fig. 2 shows the chemical potential as a function of the ionic strength  $I$  at three different values of the pH. Fig. 3 shows the osmotic pressure under the same conditions.

### C. STA

The next system we consider is silicotungstate (STA) in water with three different kinds of added salt: NaCl, HCl and LiCl. STA molecules are spherical, more or less, (see Fig. 2 in Ref. [22]) with an effective diameter of 1.1 nm [23, 24], so we set  $a = 0.55 \text{ nm}$ . The structural formula for the polyanion  $\text{SiW}_{12}\text{O}_{40}^{4-}$  implies a molar mass  $M_{STA} = 2874.3 \text{ g mol}^{-1}$ . We assume that the pH is low enough for the molecule to be fully dissociated, i.e.  $Z = 4$ .

We determine the well parameters  $U_A$  and  $\delta$  for the attractive interaction by fitting experimental data of the second virial coefficient in the same way as was done for lysozyme [7], except we now do not adjust  $Z_{eff}$ . The second virial coefficients for  $\text{Li}_4\text{STA}$ ,  $\text{H}_4\text{STA}$  and  $\text{Na}_4\text{STA}$  are taken from Ref. [25] and plotted in Fig. 4. In each case, the added salt is  $\text{XCl}$ , where X represents the counterion of the crystal. The values of the dimensionless parameters  $\omega = 1.80\sqrt{I}$ ,  $\xi = 0.645(Z_{eff}/(1+\omega))^2$ ,  $Z$  and  $Z_{eff}$  pertaining to the data in Fig. 4 are given in Table IV. We have set  $\delta = 0.05$ . A least-squares fit to the data represented in Fig. 4 then gives  $U_A = 3.30$ . In fact, there is a range of combinations of  $\delta$  and  $U_A$  that yield almost the identical curve as long as  $\delta \exp U_A \approx 1.36$  and  $\delta \ll 1$ , so our choice of  $\delta = 0.05$  is a bit arbitrary. This similarity with respect to the sole parameter  $\delta \exp U_A$  is in accord with our approximation for  $B_2$  give by Eq. (5).

The solubilities for  $\text{Li}_4\text{STA}$ ,  $\text{H}_4\text{STA}$  and  $\text{Na}_4\text{STA}$  have been measured by Zukoski et al. [25], where the same electrolytes are used as in the measurements of  $B_2$ . (See Tables V, VI and VII.) The volume fraction  $\eta$  of STA is given by  $\eta = SN_A v_0/M_{X_4STA}$ , where S is the solubility of STA (note that here it is given in g/ml, whereas for lysozyme it was given in g/l),  $v_0 = 4\pi a^3/3$  is the volume of an STA molecule and  $M_{X_4STA}$  is the molar mass, where X again represents the counterion in the respective cases. We have  $M_{H_4STA} = 2878.3 \text{ g mol}^{-1}$ ,  $M_{Li_4STA} = 2902.0 \text{ g mol}^{-1}$  and  $M_{Na_4STA} = 2966.2 \text{ g mol}^{-1}$ . The stickiness parameter  $\tau$  is determined by the method described in section II (see Eqs. (6)–(13)), using the values  $U_A = 3.30$  and  $\delta = 0.05$ . The chemical potential and the osmotic pressure are again determined from Eqs. 15 and 14 respectively. (See Tables V, VI and VII). We display these thermodynamic variables as a function of the ionic strength in Figs. 5 and 6.

### IV. CRYSTAL MODEL: DONNAN EFFECT

Having computed the thermodynamic properties of the fluid phases of lysozyme and STA, and hence those of the respective crystal phases under the assumption of equilibrium of the two phases, we now attempt to gain insight into them by introducing a simple model for the crystal. In the latter the spherical particles either touch or are very close. There are thus minute "surfaces of interaction" where the forces between two nearby spheres are predominantly attractive. It is therefore reasonable to write the thermodynamic potential  $\Omega$  of a crystal of  $N$  spheres in a volume  $V$  as a superposition of attractive and electrostatic contributions to a first approximation

$$\Omega = \frac{1}{2} k(c) \frac{(V - V_0)^2}{V_0} + N f_{el}(c, I_c) + \Pi(S, I)V - \mu(S, I)N \quad (19)$$

The crystal is immersed in a large reservoir at a constant osmotic pressure  $\Pi$  and chemical potential  $\mu$  containing a saturated solution of nanospheres at a solubility  $S$  and ionic strength  $I$  ( $\Pi$  and  $\mu$  are given by Eqs. (14) and (15) respectively). The crystal has elastic properties denoted by the modulus  $k$  which depends on the density  $c = N/V$  and the crystal would have a volume  $V_0$  in the absence of electrostatic forces ( $|V - V_0| \ll V_0$ ). Actually, the form of the elastic energy is more complicated and depends on the precise crystal habit [26] but the simple harmonic form in Eq. (19) suffices for our purposes. There is a Donnan equilibrium (see below) which leads to a salt concentration  $I_c$  within the interstitial region in the crystal. We adopt a continuum approximation: the electrostatic free energy  $N f_{el}$  is computed for a lattice of charged spheres embedded in a solvent of uniform permittivity  $\epsilon$  and electrolyte concentration  $I_c$ .

At equilibrium,  $\Omega$  must be minimized ( $\partial\Omega/\partial V = 0$ ;  $\partial\Omega/\partial N = 0$ ) so that

$$\Pi \simeq \Pi_{el} - k \left( \frac{V - V_0}{V_0} \right) + \frac{1}{2} c \frac{dk}{dc} \left( \frac{V - V_0}{V_0} \right)^2 \quad (20)$$

$$\mu \simeq \mu_{el} + \frac{1}{2} \frac{dk}{dc} \left( \frac{V - V_0}{V_0} \right)^2 \quad (21)$$

We have introduced the electrostatic counterparts of the osmotic pressure and the chemical potential of a charged sphere in the crystal phase on the right hand sides of Eqs. (20) and (21). In Eq. (20) the elastic term proportional to  $k$  may easily be of order  $\Pi_{el}$  but the quadratic form is negligible. In view of the fact that  $\Pi_{el} = O(c\mu_{el})$ , we then have  $\mu \simeq \mu_{el}$  to a good approximation from Eq. (21). In effect, as we change the ionic strength of the fluid phase, the solubility  $S$  and the salt concentration  $I_c$  within the crystal readjust themselves whereas the volume  $V$  remains virtually constant. The chemical potential is modified only by virtue of the change in electrostatic shielding about a sphere in the lattice. But a substantial hydrostatic pressure may be exerted within the crystal as we decrease its volume a bit.

Next, we compute the electrostatic properties of the crystal. The colligative properties of salt-free polyelectrolytes are often addressed in terms of a cell model in which a test cylinder is surrounded by a boundary of similar symmetry on which the electric field vanishes [27]. The boundary effectively replaces the effect of the surrounding particles on the test particle. This picture is reasonable at low volume fractions but must break down at high concentrations when the electric field is highly heterogeneous. In the latter case, one of us has advocated focusing on the voidlike regions instead of on a test particle (see Ref. [28] which deals with a hexagonal lattice of DNA at very high concentrations). Thus, in a crystal of spheres we may distinguish very small regions between particles that almost touch which we view as thin boundary layers, and larger voids which we will simply approximate by spheres. (We are here concerned with spheres of high charge density which leads to counterions being "condensed". At low charge densities, it is possible to give a more general analysis; see the Appendix). Discrete charge effects should prevail when evaluating the electrostatics of the boundary layers. These energies are here assumed to be independent of the ionic strength since the relevant scales in the boundary layers are very small in crystals of nanoparticles.

We therefore first solve the Poisson-Boltzmann equation for a charged void or spherical cavity of radius  $b$  without salt and then discuss the effect of monovalent salt via a Donnan equilibrium. The charge density on the surface of the cavity is uniform and the total number of charges is  $Z$ . In view of electroneutrality there are  $Z$  counterions in the cavity, each bearing charge  $-q$ . Within a mean-field analysis, the counterion density  $\rho(r)$  inside the cavity is given by a Boltzmann distribution in terms of the electrostatic potential  $\Psi(r)$  at a distance  $r$  from its center

$$\rho(r) = \bar{\rho} e^{q\Psi/k_B T}. \quad (22)$$

We choose  $\Psi = 0$  at the center of the cavity so that  $\bar{\rho}$  is the actual charge density there. The charge density  $-q\rho$  is also related to  $\Psi$  by Poisson's equation

$$\Delta\Psi = \frac{4\pi q\rho}{\epsilon} \quad (23)$$

leading to the Poisson-Boltzmann equation [27] which we conveniently express in the scaled form

$$\psi''(x) + \frac{2}{x}\psi'(x) = e^\psi. \quad (24)$$

Here, we have defined  $\lambda^{-2} \equiv 4\pi Q\bar{\rho}$ ,  $x \equiv r/\lambda$  and  $\psi \equiv q\Psi/k_B T$  where  $\lambda$  may be interpreted as a screening length. The two additional boundary conditions are

$$\psi'(0) = 0 \quad (25)$$

owing to symmetry, and

$$\frac{b}{\lambda} \psi' \left( \frac{b}{\lambda} \right) = \Lambda \equiv \frac{QZ}{b} \quad (26)$$

signifying the relation between the electric field and the charge density at the surface of the cavity.

For small  $x$ , Eq. (24) admits a series expansion  $\psi(x) = Ax^2 + Bx^4 + \dots$  with  $A = 1/6$  and  $B = O(1)$  independent of the value of the dimensionless variable  $\Lambda$ . As  $\Lambda$  tends to zero, Eq. (26) reduces to the condition of electroneutrality.

Electrostatic screening vanishes in this limit and there are no counterions "condensed" on the surface of the sphere. It is straightforward to solve Eq. (24) numerically starting with  $\psi(x) \rightarrow \frac{1}{6}x^2$  as  $x \rightarrow 0$ . We have fitted the solution to the convenient approximation

$$\psi(x) \approx -2 \ln \left( 1 - \frac{x^2}{12} - \frac{x^4}{1440} - \frac{x^6}{45330.3} \right), \quad (27)$$

which is accurate to within 0.6 % for  $0 \leq x \leq 3.273687$  ( $\psi(x)$  diverges at  $x \approx 3.27368734$ ). This leads to an effective charge given by

$$Z_{eff} \equiv \frac{4\pi b^3 \bar{\rho}}{3} = \frac{Z}{3\Lambda} \left( \frac{b}{\lambda} \right)^2. \quad (28)$$

This is always less than the actual charge  $Z$  which one may interpret as a certain fraction of counterions being associated near the surface if  $\Lambda > 0$ . The effective charge  $Z_{eff}$  tends to  $Z$  as  $\Lambda \rightarrow 0$  (for a general analysis of this limit, see the Appendix).

We now wish to analyze the thermodynamic properties of the crystal in the presence of simple salt which we do within a Donnan approximation. At this stage it is well to recall the incorrectness of applying Donnan arguments to a fluid of charged colloidal particles. The probability of the double layers of two particles interpenetrating is very small owing to Boltzmann weighting. Hence, only the Debye-Hückel tails in their interaction are important which represent effectively the potential of mean force between the particles. In the case of excess salt, we then use the McMillan-Mayer theory to calculate the statistical mechanical properties of the fluid as has been done in section II (see Eq. (2); this line of argumentation goes back to Stigter [29]). The situation is decidedly different when the particles are positionally ordered as in a crystal. The double layers are forced to overlap in that case. A usual (Donnan) approximation is then to suppose those points at zero electric field are in equilibrium with the reservoir [27]. For the cavities in the crystal, this yields

$$I_c(\bar{\rho} + I_c) = I^2 \quad (29)$$

in view of the equality of the chemical potentials of the small ions in the respective phases. The osmotic pressure is given by the additivity rule as argued by Oosawa for polyions within conventional cell models [27]

$$\begin{aligned} \Pi &= (\bar{\rho} + 2I_c - 2I)k_B T \\ &= \bar{\rho} k_B T [\sqrt{1 + w^2} - w] \end{aligned} \quad (30)$$

$$w \equiv \frac{2I}{\bar{\rho}}.$$

The ions have been considered as ideal and the electrostatic stress is zero in Eq. (20). The chemical potential of the charged cavity, accurate to the same level of approximation, is readily computed from Eq. (30) (this is analogous to similar calculations for cell models of long charged rods [30])

$$\mu = \mu_{ref} + \frac{Z_{eff} k_B T}{2} \ln \left[ \frac{\sqrt{1 + w^2} + 1}{\sqrt{1 + w^2} - 1} \right] \quad (31)$$

where  $\mu_{ref}$  is a reference chemical potential independent of the concentration of salt, and not identical with  $\mu_0$  of section II. Because the number of particles in the crystal is equal to the number of cavities, Eq. (31) also represents the chemical potential of a charged sphere carrying  $Z$  charges but with a different  $\mu_{ref}$ .

## A. Comparison with experiment

### 1. Lysozyme crystal

The volume per lysozyme molecule in the tetragonal crystal is  $29.7 \text{ nm}^3$  (see section III.B). The radius of the effective sphere is  $1.61 \text{ nm}$  so the volume of a cavity is  $12.2 \text{ nm}^3$  and  $b = 1.43 \text{ nm}$ . In Tables VIII-X, we show values of  $Z$  as a function of the ionic strength  $I$  at three values of the pH. From these we calculate the dimensionless quantities  $\Lambda$ ,  $b/\lambda$  and  $Z_{eff}$  via the Poisson-Boltzmann equation. Then the pressure and the chemical potential are evaluated using Eqs. (30) and (31). (See Tables VIII-X). The curves in Fig. 7 represent the chemical potential computed in this manner together with the predictions from the theory of the liquid state as displayed in Fig.2. The former have been shifted by an amount which is unknown in the present theory.

## 2. STA crystals

In order to compute the chemical potential we first need to discuss the crystal habits of STA. It is known that  $H_4STA$  is fully dissociated for a pH larger than 5 [31]. Zukoski et al. [5, 25, 32] fail to mention the pH at which their measurements were performed, though they did deduce that all forms of STA are dissociated in their experiments judging from the conductivities of their solutions.

### a. $H_4STA.31H_2O$

This crystallizes at room temperature [33] in the tetragonal form (long axis = 1.856 nm, short axes = 1.301 nm [34]; there are 2 STA molecules per unit cell of  $3.142 \text{ nm}^3$ ). We have earlier set the radius of an STA ion equal to 0.55 nm (see section III.C) so the volume of  $H_2O$  per STA molecule is  $0.874 \text{ nm}^3$  or  $b = 0.593 \text{ nm}$ . In Refs. [5] and [32] the water content of this crystal is given in terms of the molecular formula  $H_4STA.31H_2O$ .

### b. $Li_4STA.24H_2O/Li_4STA.26H_2O$

Kraus describes two forms of  $Li_4STA$  with 24  $H_2O$  and 26  $H_2O$  molecules attached respectively [35]. Both crystals are rhombohedral (short axes in both cases = 1.559 nm, long axis = 3.898 nm in the former, long axis = 4.118 nm in the latter; the angle between the short axes =  $120^\circ$  [34]). Kraus also mentions that one Li ion should probably be replaced by one H ion. There are actually three different numbers quoted for the water content of  $Li_4STA.nH_2O$  in Refs. [5, 25, 32]:  $n = 21, 24$  and  $26$ ! We have opted for  $n = 25$ , namely the average number for the crystal habits generally accepted. As there are 6 STA molecules per unit cell, the volume of crystal per STA molecule is  $1.406 \text{ nm}^3$  and the radius of our effective cavity is  $b = 0.553 \text{ nm}$ .

### c. $Na_4STA.18H_2O$

This crystallizes in the triclinic form within a narrow range around 308 K [33]. The absolute dimensions of the unit cell do not seem to be known. We thus estimate the amount of  $H_2O$  per STA molecule via the molecular formulas. The water content in  $Na_4STA.nH_2O$  is stated to be  $n = 18$  in Ref. [32] and  $n = 14$  in Ref. [5]. The latter value seems too low and is possibly a misprint since  $n$  should be equal to 20 according to the usual citation [36]. Accordingly, we adopt  $n = 18$  here to be used in the solubility studies [25]. A molecule of  $H_2O$  has a volume of  $0.0285 \text{ nm}^3$  which is based on the amount of  $H_2O$  in the unit cells of  $H_4STA.31H_2O$  and  $Li_4STA.26H_2O$ . Therefore,  $Na_4STA.18H_2O$  has  $0.513 \text{ nm}^3$   $H_2O$  per STA molecule so we have  $b = 0.496 \text{ nm}$ .

Overall, it is not clear how much  $H_2O$  is exactly present in the STA crystals. Fortunately, the chemical potential (Eq. (31)) depends only logarithmically on this quantity so the data compiled in Tables XI-XIII are not so sensitive to this type of uncertainty. The predicted chemical potentials are depicted as curves in Fig. 8 together with the computations from our theory of the liquid state (Fig. 5).

## V. DISCUSSION

Except for a slight downward adjustment of the effective charge of lysozyme in the fluid phase, there are essentially no adjustable parameters in our analysis. The adhesion parameters are completely constrained by the 2nd virial curves (Figs. 1 and 4). We predict that the chemical potentials in the fluid and solid phases should coincide apart from an unimportant shift in the vertical offset because the reference potential is not known exactly for the crystal. This appears to be almost the case for lysozyme (see Fig. 7) but there is an appreciable disparity between the respective curves in the case of the silicotungstates (see Fig. 8). Nevertheless, we note that the shapes of the curves are the same which implies that the logarithmic form in Eq. (31) appears to be confirmed i.e. the Donnan effect seems to apply to crystals of charged nanoparticles. This is borne out by adjusting  $Z_{eff}$  upward somewhat for both types of crystals. We then actually attain coincident curves (see Figs. 7 and 8). A further implication is that the precise crystal structure is unimportant with regard to the ionic-strength dependence of  $\mu$ . Eq. (31) results from approximating the cavities within the crystals by spheres; the detailed electrostatics is independent of the salt concentration.

The coexistence equation for the osmotic pressure yields little information (see Eq. (20)) because it is unclear how to relate the adhesive forces between spheres to the elastic properties of the crystal. To compute the latter we



need insight in the forces between the particles at the Ångström level which we do not have at present. Adhesive interactions appear to play a minor role in the STA crystals for the fluid and crystal pressures are quite close (compare Tables V-VII with XI-XIII). By contrast, in lysozyme crystals the osmotic pressure due to electrostatic forces is largely balanced by sticky interactions between touching protein molecules.

It is wise to emphasize the shortcomings in the approximations introduced in the electrostatic interactions. Discrete charge effects have been disregarded entirely. At the same level of approximation we have not addressed the electrostatics of the minutely thin boundary layers between almost touching spheres within the crystal phase. There are cavities at nanometer scales and these are assumed to give rise to the ionic-strength dependence of the free energy of the crystal. The Donnan approximation used suffers from the same drawback as always: the effective charge  $Z_{eff}$  is posited to be independent of the electrolyte in the crystal and thus the reservoir (the fluid phase in our case). It would be interesting to study the fluid-crystal coexistence of globular particles of low charge density. The counterions in the crystal would then be essentially free (see the Appendix) and there would be less uncertainty about the magnitude of the electrostatic interactions.

There is another potential problem in the fluid phases of silicotungstates. At 1 M electrolyte, the solubilities of STA are remarkably high (see Tables V-VII). It would appear that the counterions arising from STA should contribute to the screening on a par with the salt ions. This is not borne out by the present analysis, however, since there is no levelling off of the chemical potentials in the crystal phases in Figs. 7 and 8. Nevertheless, a liquid state theory of concentrated charged nanoparticles needs to be developed in which the counterions are duly accounted for. We note that the interaction between the particles is not pairwise additive in that case.

In summary, we have provided a semi-quantitative explanation for the ionic-strength dependence of the fluid-crystal coexistence of suspensions of charged nanoparticles. We believe this explanation is especially forceful because we have considered two rather disparate types of globular particles in detail. In particular, the solubility curves of lysozyme and silicotungstate differ markedly, yet the curves for the chemical potentials turn out to have the same form.

## VI. APPENDIX: POISSON-BOLTZMANN EQUATION IN A CRYSTAL OR POROUS MEDIUM

It is possible to present a general analysis of the Poisson-Boltzmann equation for the electrostatic potential  $\Psi(\vec{r})$  at position  $\vec{r}$  within the aqueous interstitial space inside a crystal (which may be considered to be a porous medium), under appropriate conditions. The particles in the crystal are positively charged and simple salt is absent at first. The potential is again related to the counterion density  $\rho(\vec{r})$  via the Poisson Eq. (23). Now it is possible to discern some point  $P$  in the void between several particles where the potential is a local minimum and where the density is  $\bar{\rho}_P(0)$  (see Fig. 9). Point  $P$  is chosen as the origin.

If the potential is scaled analogously as in section IV, we have  $\rho(\vec{r}) = \bar{\rho}_P \exp \psi(\vec{r})$  (see Eq. (22)). Thus, the Poisson-Boltzmann equation may be written as

$$\Delta \psi = \lambda_P^{-2} e^\psi \quad (32)$$

where the screening length  $\lambda_P$  is given by  $\lambda_P^{-2} = 4\pi Q \bar{\rho}_P$ .

In general, it is difficult to address Eq. (32) because  $\lambda_P$  is unknown. But it is possible to progress if we suppose  $|\vec{d}| \lesssim \lambda_P$  where  $|\vec{d}|$  is the largest vector distance between  $P$  and a point on the surface of the surrounding spheres (i.e. those belonging to a cluster enclosing the void centered on  $P$ ). A solution of Eq. (32) must have the form  $\psi(\vec{r}/\lambda_P)$  and may be written as a Taylor expansion to second order

$$\psi(\vec{r}) = \frac{1}{2} \vec{r} \vec{r} : \left. \frac{\partial^2 \psi}{\partial \vec{r} \partial \vec{r}} \right|_{\vec{r}=0} \quad (33)$$

if  $|\vec{d}| \lesssim \lambda_P$ . Next, we have a boundary condition on the electric field at  $\vec{r} = \vec{d}$

$$\vec{n} \cdot \left. \frac{\partial \psi}{\partial \vec{r}} \right|_{\vec{r}=\vec{d}} = \vec{n} \vec{d} : \left. \frac{\partial^2 \psi}{\partial \vec{r} \partial \vec{r}} \right|_{\vec{r}=0} = 4\pi k_1 \sigma_b Q. \quad (34)$$

Here,  $\sigma_b$  is the uniform density of charge on a sphere and  $k_1$  is a numerical coefficient of order unity. The effect of an internal permittivity is disregarded. The left-hand side of Eq. (34) scales as  $\lambda_P^{-2}$  implying that  $\bar{\rho}_P$  must be proportional to  $\sigma_b$ . In view of electroneutrality we also require the average of  $\rho(\vec{r})$  to be proportional to  $\sigma_b$ . Hence, the potential  $\psi(\vec{r})$  must be very small, which is consistent with the initial Ansatz Eq. (33). We conclude that for small enough cavitylike voids, the density of counterions is approximately constant so that the effective charge density is virtually equal to the actual charge density. In that case, when the crystal is immersed in a reservoir containing monovalent electrolyte, Eqs. (30) and (31) are valid with  $\bar{\rho}$  simply given by the concentration of counterions in the

interstitial space between the spheres;  $Z_{eff} = Z$  in Eq. (31). Because  $|\bar{d}| = O(a)$ , we ultimately require  $ZQ/a \ll 1$  as a necessary and sufficient condition for this to hold true. In the spherical cavity approximation introduced in Section IV, we have  $b = O(a)$  so  $\Lambda \ll 1$  is effectively the same requirement (which led to  $Z_{eff} = Z$ ).

- 
- [1] A. George and W.W. Wilson, *Acta Crystallogr.* **D50**, 361 (1994).  
[2] A. George, Y. Chiang, B. Guo, A. Arabshahi, Z. Cai and W.W. Wilson, *Methods Enzymol.* **276**, 100 (1997).  
[3] B. Guo, S. Kao, H. McDonald, A. Asanov, L.L. Combs and W.W. Wilson, *J. Cryst. Growth* **196**, 424 (1999).  
[4] C. Haas, J. Drenth and W.W. Wilson, *J. Phys. Chem. B* **103**, 2808 (1999).  
[5] D. Rosenbaum, P.C. Zamora and C.F. Zukoski, *Phys. Rev. Lett.* **76**, 150 (1996).  
[6] D.F. Rosenbaum and C.F. Zukoski, *J. Cryst. Growth* **169**, 752 (1996).  
[7] P. Prinsen and T. Odijk, *J. Chem. Phys.* **121**, 6525 (2004).  
[8] P. Prinsen, J.C. Pàmies, T. Odijk and D. Frenkel, *Application of the Optimized Baxter Model to the hard-core attractive Yukawa system*, submitted to *J. Chem. Phys.*, preprint at <http://arXiv.org/cond-mat/0603716>.  
[9] C. Haas and J. Drenth, *J. Phys. Chem. B* **102**, 4226 (1998).  
[10] C. Haas and J. Drenth, *J. Cryst. Growth* **196**, 388 (1999).  
[11] R.A. Curtis, H.W. Blanch and J.M. Prausnitz, *J. Phys. Chem. B* **105**, 2445 (2001).  
[12] E. Cacioppo and M.L. Pusey, *J. Cryst. Growth* **114**, 286 (1991).  
[13] W.C.K. Poon, S.U. Egelhaaf, P.A. Beales, A. Salonen and L. Sawyer, *J. Phys.: Condens. Matter* **12**, L569 (2000); P.B. Warren, *J. Phys.: Condens. Matter* **14**, 7617 (2002).  
[14] R.J. Baxter, *J. Chem. Phys.* **49**, 2770 (1968).  
[15] H.C. Andersen, J.D. Weeks and D. Chandler, *Phys. Rev. A* **4**, 1597 (1971).  
[16] B. Barboy, *J. Chem. Phys.* **61**, 3194 (1974).  
[17] L.K. Steinrauf, *Acta Cryst.* **12**, 77 (1959).  
[18] A. Nadarajah and M.L. Pusey, *Acta Cryst. D* **52**, 983 (1996).  
[19] V. Mikol, E. Hirsch and R. Giegé, *J. Mol. Biol.* **213**, 187 (1990).  
[20] D.E. Kuehner, J. Engmann, F. Fergg, M. Wernick, H.W. Blanch, and J.M. Prausnitz, *J. Phys. Chem. B* **103**, 1368 (1999).  
[21] M. Riès-Kautt, A. Ducruix, and A. van Dorsselaer, *Acta Cryst. D* **50**, 366 (1994).  
[22] M. Ge, A.A. Gewirth, W.G. Klemperer, and C.G. Wall, *Pure & Appl. Chem.* **69**, 2175 (1997).  
[23] M.C. Baker, P.A. Lyons, and S.J. Singer, *J. Am. Chem. Soc.* **77**, 2011 (1955).  
[24] T. Kurucsev, A.M. Sargeson, and B.O. West, *J. Phys. Chem.* **61**, 1567 (1957).  
[25] C.F. Zukoski, D.F. Rosenbaum, and P.C. Zamora, *Chem. Eng. Res. Des.* **74**, 723 (1996).  
[26] L.D. Landau and E.M. Lifshitz, *Theory of Elasticity, Third Edition*, (Pergamon, Oxford, U.K., 1986).  
[27] F. Oosawa, *Polyelectrolytes*, (Marcel Dekker, New York, 1971)  
[28] T. Odijk, *Philos. Trans. R. Soc. London, Ser. A* **362**, 1497 (2004).  
[29] D. Stigter, *Biopolymers* **16**, 1435 (1977).  
[30] T. Odijk and F. Slok, *J. Phys. Chem. B* **107**, 8074 (2003).  
[31] M.J. Kronman and S.N. Timasheff, *J. Phys. Chem.* **63**, 629 (1959).  
[32] P.C. Zamora and C.F. Zukoski, *Langmuir* **12**, 3541 (1996).  
[33] G. Wyrouboff, *Z. Krist.* **29**, 659 (1898).  
[34] H.T. Evans, *Perspectives in Structural Chemistry*, J.D. Dunitz and J.A. Ibers, Eds., Vol. IV, pp 8-21 (Wiley, New York, 1971).  
[35] O. Kraus, *Z. Krist.* **94**, 256 (1936).  
[36] *Gmelins Handbuch der anorganischen Chemie, Wolfram*, R.J. Meyer (Verlag Chemie, Berlin, 1933).

### Tables

| $I$ (%w/v) | $I$ (M) | $\omega$ | $Z$  | $Z_{eff}$ | $\bar{Z}$ | $\xi$ | $\tau$ | $S$ (g/l) | $\eta$  | $\frac{\mu - \mu_0}{k_B T}$ | $\frac{\Pi v_0}{k_B T}$ |
|------------|---------|----------|------|-----------|-----------|-------|--------|-----------|---------|-----------------------------|-------------------------|
| 2.0        | 0.40    | 3.35     | 11.1 | 10.93     | 9.93      | 1.146 | 0.138  | 48.7      | 0.0358  | -3.55                       | 0.0319                  |
| 3.0        | 0.57    | 4.00     | 11.2 | 11.07     | 10.07     | 0.893 | 0.101  | 14.0      | 0.0103  | -4.69                       | 0.0097                  |
| 4.0        | 0.74    | 4.56     | 11.4 | 11.29     | 10.29     | 0.755 | 0.087  | 4.30      | 0.00316 | -5.80                       | 0.0031                  |
| 5.0        | 0.92    | 5.05     | 11.6 | 11.51     | 10.51     | 0.663 | 0.079  | 3.11      | 0.00229 | -6.12                       | 0.0022                  |
| 7.0        | 1.26    | 5.92     | 11.7 | 11.63     | 10.63     | 0.519 | 0.070  | 1.36      | 0.00100 | -6.93                       | 0.0010                  |

TABLE I: The charge  $Z$  of hen-egg-white lysozyme (from Ref. [20]), the effective charge  $Z_{eff}$  (from Eq. 3), the lowered effective charge  $\bar{Z} = Z_{eff} - 1$ , the dimensionless interaction parameters  $\omega$ ,  $\xi$  and  $\tau$ , the solubility of lysozyme  $S$ , the volume fraction  $\eta$ , the dimensionless chemical potential  $(\mu - \mu_0)/k_B T$  and the dimensionless pressure  $\Pi v_0/k_B T$

as a function of the ionic strength  $I$  in the fluid phase. The pH equals 4.0 and  $\xi$  has been calculated using the lowered effective charge  $\bar{Z}$ .

| $I$ (%w/v) | $I$ (M) | $\omega$ | $Z$  | $Z_{eff}$ | $\bar{Z}$ | $\xi$ | $\tau$ | $S$ (g/l) | $\eta$  | $\frac{\mu-\mu_0}{k_B T}$ | $\frac{\Pi v_0}{k_B T}$ |
|------------|---------|----------|------|-----------|-----------|-------|--------|-----------|---------|---------------------------|-------------------------|
| 2.0        | 0.40    | 3.35     | 10.2 | 10.07     | 9.07      | 0.956 | 0.114  | 30.1      | 0.0221  | -4.02                     | 0.0199                  |
| 3.0        | 0.57    | 4.00     | 10.3 | 10.20     | 9.20      | 0.745 | 0.089  | 10.3      | 0.00759 | -4.99                     | 0.0072                  |
| 4.0        | 0.74    | 4.56     | 10.3 | 10.22     | 9.22      | 0.606 | 0.078  | 5.22      | 0.00385 | -5.63                     | 0.0037                  |
| 5.0        | 0.92    | 5.05     | 10.4 | 10.33     | 9.33      | 0.523 | 0.072  | 3.43      | 0.00253 | -6.03                     | 0.0025                  |
| 7.0        | 1.26    | 5.92     | 10.4 | 10.35     | 9.35      | 0.401 | 0.065  | 1.87      | 0.00137 | -6.62                     | 0.0014                  |

TABLE II: Same as Table I, but now with a pH equal to 4.5.

| $I$ (%w/v) | $I$ (M) | $\omega$ | $Z$ | $Z_{eff}$ | $\bar{Z}$ | $\xi$ | $\tau$ | $S$ (g/l) | $\eta$  | $\frac{\mu-\mu_0}{k_B T}$ | $\frac{\Pi v_0}{k_B T}$ |
|------------|---------|----------|-----|-----------|-----------|-------|--------|-----------|---------|---------------------------|-------------------------|
| 2.0        | 0.40    | 3.35     | 9.1 | 9.00      | 8.00      | 0.745 | 0.094  | 17.6      | 0.0130  | -4.52                     | 0.0119                  |
| 3.0        | 0.57    | 4.00     | 9.1 | 9.03      | 8.03      | 0.568 | 0.077  | 7.38      | 0.00543 | -5.31                     | 0.0052                  |
| 4.0        | 0.74    | 4.56     | 9.2 | 9.14      | 8.14      | 0.473 | 0.070  | 4.72      | 0.00347 | -5.73                     | 0.0034                  |
| 5.0        | 0.92    | 5.05     | 9.2 | 9.15      | 8.15      | 0.399 | 0.066  | 3.63      | 0.00267 | -5.98                     | 0.0026                  |
| 7.0        | 1.26    | 5.92     | 9.1 | 9.07      | 8.07      | 0.299 | 0.060  | 2.46      | 0.00181 | -6.36                     | 0.0018                  |

TABLE III: Same as Table I, but now with a pH equal to 5.4.

| $I$ (M) | $\omega$ | $Z$  | $Z_{eff}$ | $\xi$ |
|---------|----------|------|-----------|-------|
| 0.3     | 0.99     | 4.00 | 3.42      | 1.905 |
| 1.0     | 1.80     | 4.00 | 3.58      | 1.054 |
| 3.0     | 3.13     | 4.00 | 3.76      | 0.536 |
| 4.0     | 3.61     | 4.00 | 3.80      | 0.439 |
| 5.0     | 4.03     | 4.00 | 3.83      | 0.373 |

TABLE IV: Values of the bare charge  $Z$  of STA, the effective charge  $Z_{eff}$  (from Eq. (3)) and the dimensionless interaction parameters  $\omega = 1.80\sqrt{I}$  and  $\xi = 0.645(Z_{eff}/(1+\omega))^2$  as a function of the ionic strength  $I$ . These entries apply to the data plotted in Fig. 4.

| $I$ (M) | $\omega$ | $Z$ | $Z_{eff}$ | $\xi$ | $\tau$ | $S$ (g/ml) | $\eta$ | $\frac{\mu-\mu_0}{k_B T}$ | $\frac{\Pi v_0}{k_B T}$ |
|---------|----------|-----|-----------|-------|--------|------------|--------|---------------------------|-------------------------|
| 1.0     | 1.80     | 4.0 | 3.58      | 1.054 | 0.786  | 1.94       | 0.284  | 1.30                      | 0.706                   |
| 2.0     | 2.55     | 4.0 | 3.70      | 0.700 | 0.358  | 1.67       | 0.243  | -0.48                     | 0.375                   |
| 3.0     | 3.13     | 4.0 | 3.76      | 0.536 | 0.255  | 1.36       | 0.198  | -1.40                     | 0.226                   |
| 4.0     | 3.61     | 4.0 | 3.80      | 0.439 | 0.215  | 1.11       | 0.162  | -1.91                     | 0.158                   |
| 5.0     | 4.03     | 4.0 | 3.83      | 0.373 | 0.193  | 0.57       | 0.0830 | -2.65                     | 0.077                   |

TABLE V: The charge  $Z$  of STA, the effective charge  $Z_{eff}$  (from Eq. (3)), the dimensionless interaction parameters  $\omega$ ,  $\xi$  and  $\tau$ , the solubility  $S$  of H<sub>4</sub>STA, the volume fraction  $\eta$ , the dimensionless chemical potential  $(\mu - \mu_0)/k_B T$  and the dimensionless pressure  $\Pi v_0/k_B T$  as a function of the ionic strength  $I$  in the fluid phase. Here the counterion is H<sup>+</sup> and the added salt is HCl.  $\xi$  has been calculated using the effective charge  $Z_{eff}$ .

| $I$ (M) | $\omega$ | $Z$  | $Z_{eff}$ | $\xi$ | $\tau$ | $S$ (g/ml) | $\eta$ | $\frac{\mu-\mu_0}{k_B T}$ | $\frac{\Pi v_0}{k_B T}$ |
|---------|----------|------|-----------|-------|--------|------------|--------|---------------------------|-------------------------|
| 1.0     | 1.80     | 4.00 | 3.58      | 1.054 | 0.668  | 2.15       | 0.312  | 1.55                      | 0.811                   |
| 2.0     | 2.55     | 4.00 | 3.70      | 0.700 | 0.352  | 1.85       | 0.267  | -0.26                     | 0.433                   |
| 3.0     | 3.13     | 4.00 | 3.76      | 0.536 | 0.255  | 1.36       | 0.197  | -1.41                     | 0.224                   |
| 4.0     | 3.61     | 4.00 | 3.80      | 0.439 | 0.215  | 0.81       | 0.118  | -2.23                     | 0.114                   |
| 5.0     | 4.03     | 4.00 | 3.83      | 0.373 | 0.193  | 0.32       | 0.0469 | -3.16                     | 0.045                   |

TABLE VI: Same as Table V, but now with  $\text{Li}^+$  as counterion and  $\text{LiCl}$  as added salt.

| $I$ (M) | $\omega$ | $Z$ | $Z_{eff}$ | $\xi$ | $\tau$ | $S$ (g/ml) | $\eta$ | $\frac{\mu-\mu_0}{k_B T}$ | $\frac{\Pi v_0}{k_B T}$ |
|---------|----------|-----|-----------|-------|--------|------------|--------|---------------------------|-------------------------|
| 1.0     | 1.80     | 4.0 | 3.58      | 1.054 | 0.906  | 1.85       | 0.262  | 1.07                      | 0.625                   |
| 2.0     | 2.55     | 4.0 | 3.70      | 0.700 | 0.359  | 1.67       | 0.236  | -0.54                     | 0.358                   |
| 3.0     | 3.13     | 4.0 | 3.76      | 0.536 | 0.255  | 1.36       | 0.192  | -1.44                     | 0.218                   |
| 4.0     | 3.61     | 4.0 | 3.80      | 0.439 | 0.215  | 0.74       | 0.104  | -2.35                     | 0.100                   |
| 5.0     | 4.03     | 4.0 | 3.83      | 0.373 | 0.193  | 0.46       | 0.0657 | -2.86                     | 0.062                   |

TABLE VII: Same as Table V, but now with  $\text{Na}^+$  as counterion and  $\text{NaCl}$  as added salt.

| $I$ (%w/v) | $I$ (M) | $Z$  | $\Lambda$ | $b/\lambda$ | $Z_{eff}$ | $w$  | $\frac{\mu}{k_B T}$ | $\frac{\Pi v_0}{k_B T}$ |
|------------|---------|------|-----------|-------------|-----------|------|---------------------|-------------------------|
| 2.0        | 0.40    | 11.1 | 5.51      | 2.52        | 4.27      | 1.39 | 2.87                | 1.97                    |
| 3.0        | 0.57    | 11.2 | 5.56      | 2.53        | 4.29      | 1.97 | 2.10                | 1.47                    |
| 4.0        | 0.74    | 11.4 | 5.66      | 2.54        | 4.32      | 2.54 | 1.66                | 1.17                    |
| 5.0        | 0.92    | 11.6 | 5.76      | 2.55        | 4.35      | 3.10 | 1.38                | 0.98                    |
| 7.0        | 1.26    | 11.7 | 5.81      | 2.55        | 4.36      | 4.24 | 1.02                | 0.72                    |

TABLE VIII: The ionic strength  $I$ , the actual number of charges  $Z$ , the effective number  $Z_{eff}$ , the chemical potential  $\mu$  and the osmotic pressure  $\Pi$  for a lysozyme crystal at pH 4.0 (the reference chemical potential has been set equal to zero).

| $I$ (%w/v) | $I$ (M) | $Z$  | $\Lambda$ | $b/\lambda$ | $Z_{eff}$ | $w$  | $\frac{\mu}{k_B T}$ | $\frac{\Pi v_0}{k_B T}$ |
|------------|---------|------|-----------|-------------|-----------|------|---------------------|-------------------------|
| 2.0        | 0.40    | 10.2 | 5.07      | 2.48        | 4.13      | 1.43 | 2.69                | 1.86                    |
| 3.0        | 0.57    | 10.3 | 5.12      | 2.49        | 4.15      | 2.04 | 1.96                | 1.38                    |
| 4.0        | 0.74    | 10.3 | 5.12      | 2.49        | 4.15      | 2.64 | 1.53                | 1.08                    |
| 5.0        | 0.92    | 10.4 | 5.17      | 2.49        | 4.16      | 3.24 | 1.27                | 0.90                    |
| 7.0        | 1.26    | 10.4 | 5.17      | 2.49        | 4.16      | 4.45 | 0.93                | 0.66                    |

TABLE IX: Same as Table VIII, but now for pH 4.5.

| $I$ (%w/v) | $I$ (M) | $Z$ | $\Lambda$ | $b/\lambda$ | $Z_{eff}$ | $w$  | $\frac{\mu}{k_B T}$ | $\frac{\Pi v_0}{k_B T}$ |
|------------|---------|-----|-----------|-------------|-----------|------|---------------------|-------------------------|
| 2.0        | 0.40    | 9.1 | 4.52      | 2.42        | 3.93      | 1.51 | 2.45                | 1.70                    |
| 3.0        | 0.57    | 9.1 | 4.52      | 2.42        | 3.93      | 2.15 | 1.77                | 1.25                    |
| 4.0        | 0.74    | 9.2 | 4.57      | 2.43        | 3.95      | 2.77 | 1.40                | 0.99                    |
| 5.0        | 0.92    | 9.2 | 4.57      | 2.43        | 3.95      | 3.41 | 1.14                | 0.81                    |
| 7.0        | 1.26    | 9.1 | 4.52      | 2.42        | 3.93      | 4.71 | 0.83                | 0.59                    |

TABLE X: Same as Table VIII, but now for pH 5.4.

| $I$ (%w/v) | $I$ (M) | $Z$ | $\Lambda$ | $b/\lambda$ | $Z_{eff}$ | $w$   | $\frac{\mu}{k_B T}$ | $\frac{\Pi v_0}{k_B T}$ |
|------------|---------|-----|-----------|-------------|-----------|-------|---------------------|-------------------------|
| 1.0        | 0.60    | 4.0 | 4.789     | 2.452       | 1.67      | 0.629 | 2.08                | 0.738                   |
| 2.0        | 1.20    | 4.0 | 4.789     | 2.452       | 1.67      | 1.257 | 1.22                | 0.466                   |
| 3.0        | 1.81    | 4.0 | 4.789     | 2.452       | 1.67      | 1.886 | 0.85                | 0.332                   |
| 4.0        | 2.41    | 4.0 | 4.789     | 2.452       | 1.67      | 2.514 | 0.65                | 0.256                   |
| 5.0        | 3.01    | 4.0 | 4.789     | 2.452       | 1.67      | 3.143 | 0.52                | 0.207                   |

TABLE XI: Same as Table VIII but now for  $\text{H}_4\text{STA}.31\text{H}_2\text{O}$ .

| $I$ (%w/v) | $I$ (M) | $Z$ | $\Lambda$ | $b/\lambda$ | $Z_{eff}$ | $w$   | $\frac{\mu}{k_B T}$ | $\frac{\Pi v_0}{k_B T}$ |
|------------|---------|-----|-----------|-------------|-----------|-------|---------------------|-------------------------|
| 1.0        | 0.60    | 4.0 | 5.134     | 2.488       | 1.61      | 0.531 | 2.23                | 0.950                   |
| 2.0        | 1.20    | 4.0 | 5.134     | 2.488       | 1.61      | 1.062 | 1.35                | 0.626                   |
| 3.0        | 1.81    | 4.0 | 5.134     | 2.488       | 1.61      | 1.594 | 0.95                | 0.455                   |
| 4.0        | 2.41    | 4.0 | 5.134     | 2.488       | 1.61      | 2.125 | 0.73                | 0.353                   |
| 5.0        | 3.01    | 4.0 | 5.134     | 2.488       | 1.61      | 2.656 | 0.59                | 0.288                   |

TABLE XII: Same as Table VIII but now for Li<sub>4</sub>STA.25H<sub>2</sub>O.

| $I$ (%w/v) | $I$ (M) | $Z$ | $\Lambda$ | $b/\lambda$ | $Z_{eff}$ | $w$   | $\frac{\mu}{k_B T}$ | $\frac{\Pi v_0}{k_B T}$ |
|------------|---------|-----|-----------|-------------|-----------|-------|---------------------|-------------------------|
| 1.0        | 0.60    | 4.0 | 5.721     | 2.542       | 1.51      | 0.410 | 2.45                | 1.374                   |
| 2.0        | 1.20    | 4.0 | 5.721     | 2.542       | 1.51      | 0.819 | 1.55                | 0.970                   |
| 3.0        | 1.81    | 4.0 | 5.721     | 2.542       | 1.51      | 1.229 | 1.12                | 0.728                   |
| 4.0        | 2.41    | 4.0 | 5.721     | 2.542       | 1.51      | 1.639 | 0.87                | 0.575                   |
| 5.0        | 3.01    | 4.0 | 5.721     | 2.542       | 1.51      | 2.049 | 0.71                | 0.473                   |

TABLE XIII: Same as Table VIII but now for Na<sub>4</sub>STA.18H<sub>2</sub>O.

### Figure Captions

FIG. 1. The second virial coefficient of lysozyme as a function of the ionic strength. The second virial coefficient is scaled by the hard sphere value  $B_2^{HS}$ . The data are taken from a variety of experiments; see Ref. [7] for more details. The added salt is NaCl. The solid line is a fit to the data with  $U_A = 2.89$  and  $\delta = 0.182$ .

FIG. 2. The dimensionless chemical potential of lysozyme in the fluid phase as a function of the ionic strength at pH 4.0 (diamonds), pH 4.5 (squares) and pH 5.4 (triangles). See also Tables I, II and III.

FIG. 3. The dimensionless pressure of lysozyme in the fluid phase as a function of the ionic strength at pH 4.0 (diamonds), pH 4.5 (squares) and pH 5.4 (triangles). See also Tables I, II and III.

FIG. 4. The second virial coefficient of STA as a function of the ionic strength. The second virial coefficient is scaled by the hard sphere value  $B_2^{HS}$ . The experimental data are taken from Zukoski et al. (Ref. [25]). The added salt is LiCl (diamonds), HCl (squares) and NaCl (triangles) respectively and in all cases the counterion of STA is the same as that of the salt. The solid line is a fit to the experimental data with  $U_A = 3.30$  and  $\delta = 0.05$ .

FIG. 5. The dimensionless chemical potential of STA in the fluid phase as a function of the ionic strength. The added salt is LiCl (diamonds), HCl (squares) and NaCl (triangles) respectively and in all cases the counterion of STA is the same as that of the salt. See also Tables V, VI and VII.

FIG. 6. The dimensionless pressure of STA in the fluid phase as a function of the ionic strength. The added salt is LiCl (diamonds), HCl (squares) and NaCl (triangles) respectively and in all cases the counterion of STA is the same as that of the salt. See also Tables V, VI and VII.

FIG. 7. The chemical potential of lysozyme in the fluid phase as a function of the ionic strength at pH 4.0 (diamonds), pH 4.5 (squares) and pH 5.4 (triangles) (see Fig. 2). The solid lines denote predictions from the theory of the crystalline state (Eq. (31)), with the effective charge from Table VIII-X. The shift in chemical potential in units of  $k_B T$  has been chosen to be 7.4 (light grey line, pH 4.0), 7.3 (black line, pH 4.5) and 7.15 (dark grey line, pH 5.4) respectively. Dashed line denotes the theory of the crystal for  $Z_{eff} = 5.0$  (shift = 7.9) and the dash-dotted line for  $Z_{eff} = 5.9$  (shift = 8.7).

FIG. 8. Chemical potential of STA in the fluid phase as a function of the ionic strength (see Fig. 5). Salt added: LiCl (diamonds); HCl (squares); NaCl (triangles) (counterion of STA is the same as that of the salt). Solid lines denote predictions from the theory of the crystalline state (Eq. (31)), with the effective charge from Table XI-XIII. The shift in chemical potential in units of  $k_B T$  is 2.3 (black line, H<sub>4</sub>STA.31H<sub>2</sub>O), 2.4 (dark grey line, Li<sub>4</sub>STA.25H<sub>2</sub>O) and 2.55 (light grey line, Na<sub>4</sub>STA.18H<sub>2</sub>O) respectively. Dashed line denotes predictions from the theory of the crystal for  $Z_{eff} = 2.8$  (shift = 5.5).

FIG. 9. Point  $P$  in a void of the crystal.

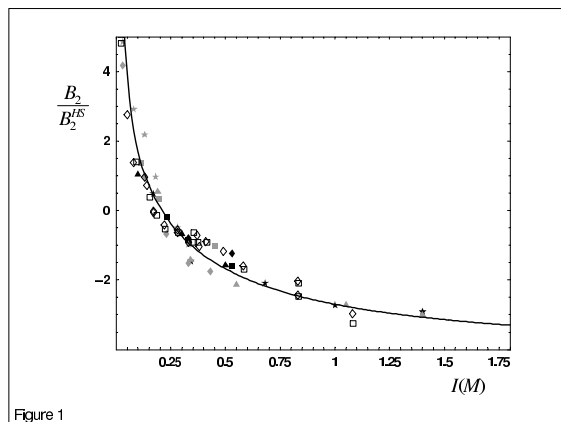


Figure 1

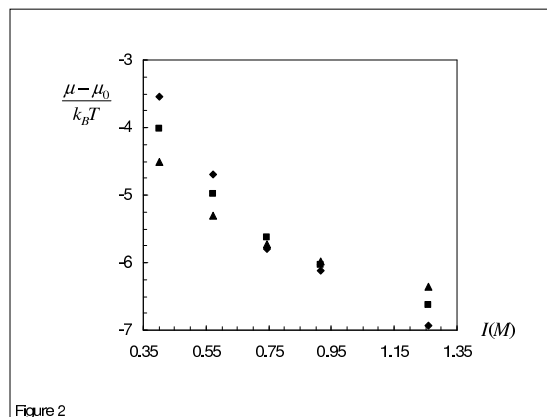


Figure 2

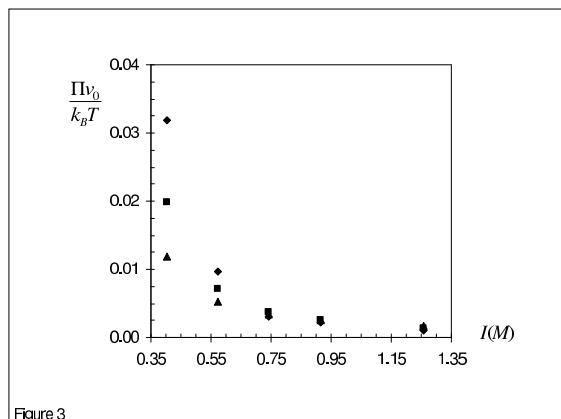


Figure 3

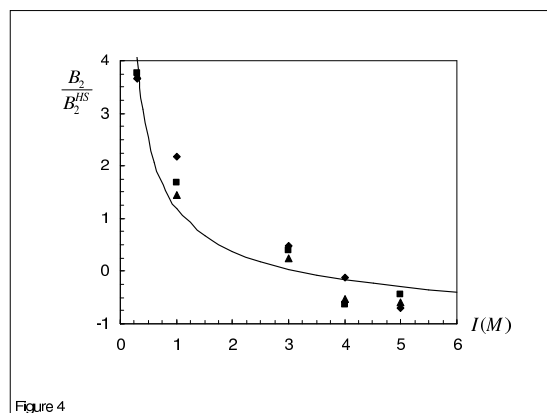


Figure 4

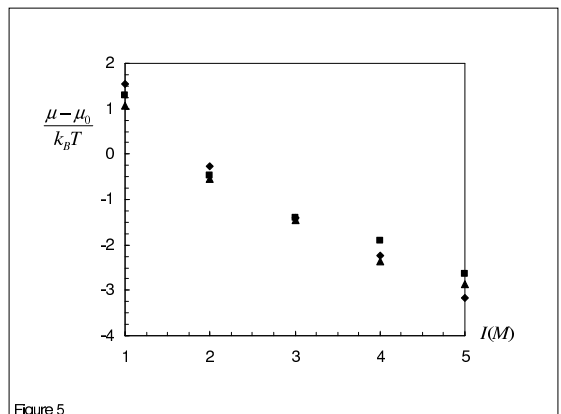


Figure 5

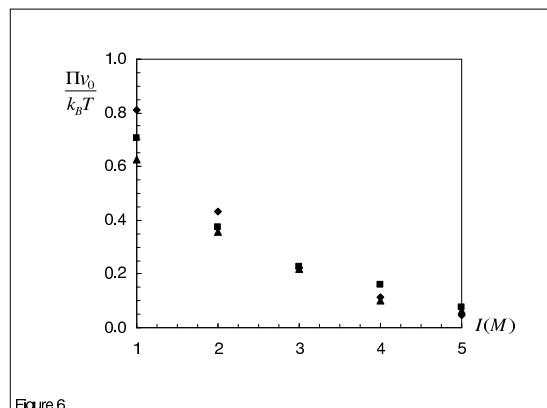


Figure 6

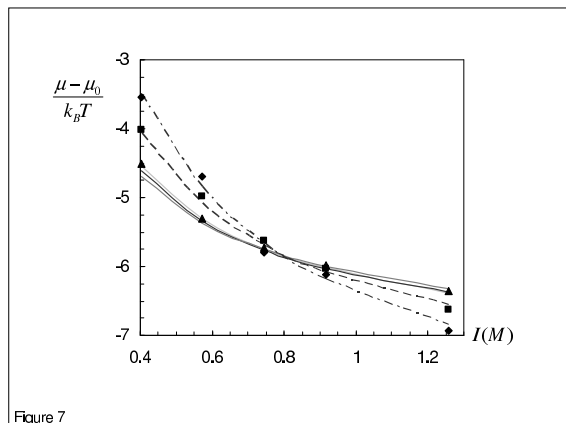


Figure 7

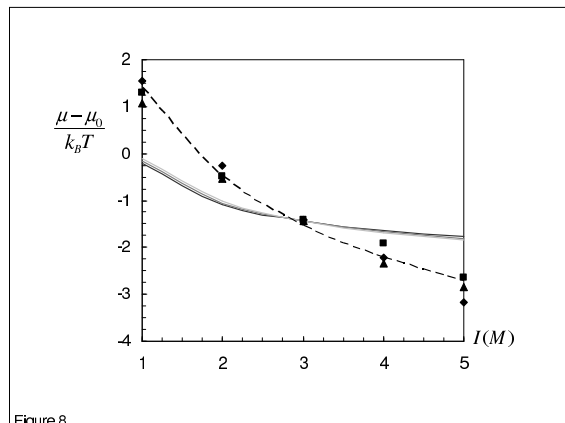


Figure 8

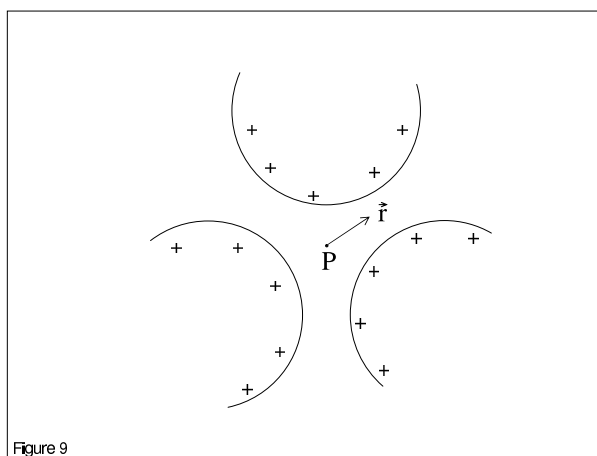


Figure 9